J Pharmacokinet Pharmacodyn
DOI 10.1007/s10928-008-9093-5

Population PK–PD model for Fc-osteoprotegerin in healthy postmenopausal women

Matthew L. Zierhut · Marc R. Gastonguay · Steven W. Martin · Paolo Vicini · Pirow J. Bekker · Donna Holloway · Philip T. Leese · Mark C. Peterson

Received: 1 March 2006 / Accepted: 5 June 2008

Abstract Osteoporosis is a metabolic bone disease resulting from increased bone resorption and characterized by low bone mass that leads to increased bone fragility and risk of fracture, particularly of the hip, spine and wrist. Bone resorption is dependent on receptor activator of NF-kappa B ligand (RANKL), which binds to RANK receptor on preosteoclasts to initiate osteoclastogenesis and maintains osteoclast function and survival. To neutralize the effects of RANKL, the body naturally produces the protein osteoprotegerin (OPG), which acts as a decoy receptor for RANKL and contributes to bone homeostasis. We describe the piecewise development of a three-compartment pharmacokinetic model with both linear and Michaelis–Menten eliminations, and an indirect pharmacodynamic response model to describe the pharmacokinetics and pharmacodynamics, respectively, of the fusion protein, Fc-osteoprotegerin (Fc-OPG), in healthy postmenopausal women. Subsequently, model verification was performed and used to address study design questions via simulation. The model was developed

M. L. Zierhut · P. Vicini
Department of Bioengineering, University of Washington,
P.O. Box 352255, Seattle, WA 98195-2255, USA

M. R. Gastonguay
Metrum Research Group LLC, Tariffville, CT 06081, USA

S. W. Martin
Pfizer Global Research & Development, Sandwich, Kent CT13 9NJ, UK

P. J. Bekker
Medical and Clinical Affairs, ChemoCentryx, Inc., Mountain View, CA 94043, USA

D. Holloway · M. C. Peterson (✉)
Amgen Inc., One Amgen Center Drive, Thousand Oaks, CA 91320, USA
e-mail: mark.peterson@biogenidec.com

P. T. Leese
Quintiles, Lenexa, KS 66219, USA

using data from eight cohorts (n = 13 subjects/cohort; Fc-OPG:placebo = 10:3) classified by dose level (0.1, 0.3, 1.0, or 3.0 mg/kg) and route of administration (intravenous [IV] or subcutaneous [SC]). Fc-OPG serum concentrations and urinary N-telopeptide/creatinine ratios (NTX) following both IV and SC administration were available. The model provided an adequate fit to the observed data and physiologically plausible parameter estimates. Model robustness was tested via a posterior predictive check with the model performing well in most cases. Subsequent clinical trial simulations demonstrated that a single 3.0-mg/kg SC dose of Fc-OPG would be expected to produce, at 14 days post-dose, a median NTX percentage change from baseline of −45% (with a 95% prediction interval ranging from −34% to −60%). Lastly, model ruggedness was evaluated using local and global sensitivity analysis methods. In conclusion, the model selection and simulation strategies we applied were rigorous, useful, and easily generalizable.

Keywords Population PK–PD model · Fc-osteoprotegerin · RANKL · Osteoporosis · Postmenopausal women · Model evaluation · Urinary N-telopeptide

Abbreviations

DV	Dependent variable
FO	First-order
FOCE	First-order conditional estimation
IPRED	Individual model prediction
MOFV	Minimum objective function value
PRED	Population model prediction
WRES	Weighted residuals
OPG	Osteoprotegerin
RANKL	Receptor activator of NF-kappa B ligand
Fc-OPG	Fc fused to OPG molecule
NTX	Urinary N-telopeptide/creatinine ratio

Introduction

Osteoporosis is a metabolic bone disease characterized by low bone mass and deterioration of bone tissue that leads to increased bone fragility and risk of fracture, particularly of the hip, spine and wrist. It is estimated that one in four women over the age of 50 has osteoporosis, and more than 1 in 5 people who have a hip fracture will die in the first year after the fracture. As a result, osteoporosis is recognized as a major public health problem [1], with a variety of drug treatments available, including: bisphosphonates [2], hormone replacement therapy [3], selective estrogen receptor modulators [4] and anabolic parathyroid hormone [5] .

Osteoporosis is believed to be the result of increases in bone resorption over bone formation, due to both increases in osteoclastogenesis and decreased osteoclast apoptosis. Three members of the tumor necrosis factor (TNF) ligand and receptor-signaling family, receptor activator of NF-kappa B ligand (RANKL), RANK receptor, and osteoprotegerin (OPG) have been shown to be the final effectors of bone resorption

and osteoclastogenesis [6]. RANKL, the primary mediator of osteoclast formation, function, and survival, is expressed by bone marrow stromal cells and osteoblasts. It binds to RANK receptor on both preosteoclasts and mature osteoclasts to initiate osteoclastogenesis and maintain resorptive activity, respectively. RANKL activity is opposed by OPG, a protein produced by the body that acts as a decoy receptor for RANKL. OPG inhibits osteoclast activity by preventing RANKL from binding to RANK on the surface of precursor and mature osteoclasts, and contributes to the natural maintenance of bone homeostasis [6]. The inhibition of the RANKL/RANK interaction represents a promising intervention point for the treatment of osteoporosis and other bone diseases characterized by increased bone resorption, and compounds that inhibit RANKL are promising therapeutic candidates [7].

In a phase 1 study in healthy postmenopausal women, a single SC injection of a genetically engineered fusion molecule, comprising an Fc-fragment (IgG_1 derived) and OPG (Fc-OPG), which retained its binding affinity for RANKL, was effective in rapidly and profoundly reducing the bone resorption marker, urinary N-telopeptide/creatinine ratio (NTX) following dosing and by 14% at 6 weeks [8]. Using the serum Fc-OPG concentration data, NTX data, and limited covariate information from the phase 1 dose-ranging study with Fc-OPG, we developed an integrated population PK–PD model to describe the disposition of Fc-OPG following IV or SC administration, which includes mechanistic components for Fc-OPG distribution and its effects on bone resorption. We subsequently utilized the model to simulate conditions of interest pertaining to dose selection and dosing frequency that might be further investigated in clinical studies.

There are multiple reasons for developing an integrated PK–PD pharmacostatistical model. With respect to recent developments in biomarker analysis [9], this type of model may summarize available information on the mechanism of action of a drug in a quantitative and testable framework [10]. Moreover, robust, mechanistic models [11] are useful for predictive purposes, in that they may be used for simulating in silico clinical trial outcomes, and thus, evaluating competitive designs [12]. These types of models essentially support answers to question such as: "Given my current state of knowledge, what is the range of probable outcomes?" In the literature, there are numerous examples in which modeling and simulation contributed to the understanding of a mechanism of action, and thus accelerated the development process [12–15]. The FDA Guidance for Industry on Population Pharmacokinetics appropriately summarizes the utility of population PK–PD by stating that "simulating a planned study offers a potentially useful tool for evaluating and understanding the consequences of different study designs. Shortcomings in study design result in the collection of uninformative data." [16].

Specific to treatments for osteoporosis, the development of PK–PD models may provide a mechanism for facilitating efficient drug development. For ibandronate, a bisphosphonate antiresorptive compound, modeling of the PK–PD relationship was useful in designing effective treatment regimens based on prior clinical experience with a semi-mechanistic model [17]. In another case, a semi-physiologic three-compartment model described the PK of the bisphosphonate, pamidronate [18], and was subsequently linked to a PD model to adequately describe the dynamics of the bone resorption marker, hydroxyproline, following intravenous treatment. If these

models were available early in the development timeline, they could be employed to investigate study designs, select informative sampling points, and suggest commercially desirable dosing paradigms. Therefore, it is reasonable to believe that valuable time could be saved in selecting subsequent dose levels and regimens, potentially shortening the lengthy development timeline for osteoporosis treatments.

This article summarizes the development of an integrated population PK–PD model of Fc-OPG and the application of the model to relevant drug development questions through stochastic simulation. The approach is believed to be general, useful, and likely applicable to other compounds at a similar stage of development.

Materials and methods

Study design

Details on this study are available elsewhere [8]. This study was a randomized, double-blind, placebo-controlled, single-dose, dose escalation, phase 1 study of an osteoclast inhibitory compound, Fc-OPG. Eligible subjects were randomly divided into eight cohorts described by dose level (0.1, 0.3, 1.0, or 3.0 mg/kg) and route of administration (IV or SC injection). Each cohort consisted of 13 subjects who received either Fc-OPG or placebo in a 10:3 ratio, respectively. The test article used in this study consisted of a genetically engineered Fc-OPG fusion molecule that was composed of two OPG molecules bound to a single Fc-fragment (Fc-fragment of IgG1). In vitro testing demonstrated that Fc-OPG retained its binding affinity for RANKL and had similar activity as native OPG for inhibiting osteoclast differentiation. Dose solution concentrations were 10 mg/ml for the 0.1 and 0.3 mg/kg cohorts and 30 mg/ml for the 1.0 and 3.0 mg/kg cohorts. Doses of 1.0 and 3.0 mg/kg were administered as two or more bolus SC injections. Placebo consisted of only vehicle and was identical in appearance to the Fc-OPG solution.

Study subjects, pharmacokinetic (PK), and pharmacodynamic (PD) sampling

One hundred-four healthy postmenopausal women (no menses for at least 12 months) were enrolled at a single study center in Lenexa, Kansas. Study subjects were between the ages of 41 and 71 years old, ambulatory, and provided written informed consent prior to enrollment. Detailed subject demographics have been previously described by Bekker et al. [8]. Each subject was given a single dose of study drug or placebo, described by cohort, and then followed for 84 days. Serum samples were obtained and measured for Fc-OPG concentration pre-dose and at 5 min; 1, 2, 4, 8, and 12 h; and 1, 2, 3, 4, 7, 10, 14, 21, and 28 days after test article administration. Fc-OPG serum concentration determinations were made using the nOPG-Ab ELISA method (R&D Systems, Minneapolis, MN) with a limit of quantification of 0.039 ng/ml. Urine was collected for measurements of N-telopeptide and creatinine and were reported as the ratio of the two (NTX: nM BCE/mM Creatinine; Osteomark®, Seattle, WA) up to 33 days before dosing and at 1, 2, 3, 4, 7, 10, 14, 21, 28, 42, 56, 70, and 84 days after dosing.

Pharmacokinetic analysis

Initial visual inspection of raw serum Fc-OPG concentration versus time plot data prompted us to rule out one-compartment structural models. All PK analyses were then performed using a nonlinear mixed effects modeling program (NONMEM, Version V, level 1.1, ADVAN8, TRANS1) [19] on an Intel-based PC with the Compaq Visual Fortran Compiler, Version 6.6 B. Initially, various structural PK models were analyzed using a comprehensive naïve pooled data set, including data from all routes of administration. This approach was feasible because of the balanced study design. Due to convergence issues with the full dataset, however, a piecewise strategy was applied to build an acceptable model for PK analysis. Initially, only IV data were used to determine the structural model and inter-individual variance structure. Once the base IV model was selected, the estimated parameters were fixed, and a new model was created by adding a SC dosing compartment with first-order absorption. SC data were then analyzed using this expanded model.

NONMEM first-order estimation method (FO) was initially used to examine various two- and three-compartment structural PK models with multiple types of elimination from the central compartment fit to IV data alone. These models were compared using the minimum value of the objective function (MVOF) and diagnostic plots, such as population prediction (PRED) versus observed data (DV), weighted residuals versus time, weighted residuals versus PRED, and PRED and DV versus time. A minimum difference in MVOF ($\alpha = 0.01$ for a chi-square distribution, where n degrees of freedom was change in number of parameters) was used to assist in the final selection criteria, but not for hypothesis testing. All models were first analyzed using a naïve pool approach [20], estimating only the model fixed effects parameters (THETA in NONMEM, θ in this article). All of the models were subsequently analyzed with a diagonal intersubject variance matrix (OMEGA). Intersubject variability was modeled for all fixed effect parameters, P, as:

$$P_{jk} = \theta_k \exp(\eta_{jk}) \tag{1}$$

where the random effect, η_{jk}, denotes the exponential difference between the jth individual's kth parameter estimate (P_{jk}) and the population mean kth parameter estimate (θ_k), and under FO is a random variable assumed to have a mean zero and variance ω_k^2.

To allow for a true exponential residual error structure, which stabilizes the model fitting procedure in the presence of very skewed residuals over a wide range of concentration data, the natural log transformed Fc-OPG serum concentrations were used in all model-fitting procedures [21]. Residual variability was modeled as follows:

$$\ln(C_{OPGij}) = \ln(\tilde{C}_{OPGij}) + \varepsilon_{ij} \tag{2}$$

where C_{OPGij} and $\tilde{C}_{OPGij}$ are the measured and model-predicted Fc-OPG serum concentrations, respectively, for the jth subject at the ith time point, and ε_{ij} is the random residual error, assumed to have a mean of zero and a variance σ^2.

To assess the best structure for the intersubject variance (OMEGA) matrix, NONMEM first-order conditional estimation (FOCE) with interaction was used to fit the structural PK model to IV data with various non-zero diagonal OMEGA terms (ω_k^2) included. Roughly adhering to a stepwise approach, similar in technique to many common covariate selection approaches [22], we added non-zero intersubject variances to specific PK parameters one at a time. When several ω_k^2 elements were introduced one-at-a-time to the base OMEGA matrix (initially null, as in the naïve pooling approach), only the term with the largest contribution to the MOFV ($\alpha = 0.01$ chi-square distribution) was added to the model, unless numerical instabilities or nonsensical (physiologically unrealistic) estimates were observed or obtained, respectively. The new model was then used as the basis for further additions, and the above process was repeated until all diagonal OMEGA elements were investigated and additions completed. Overall, the PK model for IV data was determined based on parsimony principles, a required minimum difference in MOFV (at $\alpha = 0.01$ for a chi-square distribution), and the availability of an asymptotic covariance matrix of parameter estimates (i.e. the NONMEM $COV calculation step was required to be successful).

After we selected an acceptable PK model for IV data, an additional first-order absorption SC dosing compartment was introduced and used to fit the SC data. All previously estimated typical values and intersubject variance parameters were fixed and residual error was estimated. Covariate effects (age, body weight, serum creatinine, years post menopause) were also investigated on all model parameters; no significant trends in the covariate-parameter relationships were observed.

Pharmacodynamic analysis

Estimating under FOCE with interaction, a PD analysis was performed using the empirical Bayes individual PK parameters from the aforementioned analysis to simulate Fc-OPG serum concentrations at the exact time points of urinary NTX measurements. Simulated Fc-OPG serum concentrations were then used in an indirect pharmacological response model to describe changes in the NTX data. Under this model, baseline NTX conditions were modeled assuming steady state conditions and programmatically initialized with a unit mass administration and a scalar comprised of the ratio of the synthesis rate and the degradation rate constant. Intersubject variance terms for all PD fixed effect parameters were included in the OMEGA matrix, as well as a covariance term for two rate constants in the indirect response model. Because there was plenty of dynamic NTX data, k_{syn} and k_{deg} were both allowed to vary in the indirect response model although their ratio predicts baseline urinary NTX as well. A combination additive and proportional residual error model was applied. As with the PK model, there were no covariates included in the final PD model.

Posterior predictive check

A description of the posterior predictive check for PK–PD models has been previously described [23]. Using all the parameters estimated from the final model, 1,000 simulations of the original data set were performed with the NONMEM $SIMULATION

subroutine, using the SIMULATIONONLY option. Parameter uncertainty, as obtained from the variance-covariance matrix of the estimates (obtained from NONMEM $COVARIANCE), was implemented in these simulations as between-trial variability for all fixed- and random-effect parameters, and was modeled using normal and lognormal probability densities for fixed and random effect parameters, respectively. Standard errors for elements of OMEGA and SIGMA were used to determine an equivalent log-normally distributed parameter uncertainty distribution to avoid negative variance realizations. SC data were simulated using the residual error model previously developed for the IV data. Only the proportional component of residual error was included in the PD simulations. The simulation results were then compared to the original data set.

Simulation and sensitivity analysis

Simulating clinical trials can be very helpful in future modeling decisions and the design of clinical trial protocols [12]. In an effort to model a putative subsequent clinical trial, a population of 200 subjects (assumed all body masses = 70 kg), all given a subcutaneously administered dose of 3.0 mg/kg (reflecting cohort 4 dosage), was simulated. The cohort 4 dosing regimen was used due to its apparent support of the desired dose effectiveness criteria (50% suppression at 2 weeks post administration). It must be noted, however, that this decision does not necessarily support a clinical conclusion.

Initially, only 200 simulations of 200 subjects each were performed to display the variation in the population PD profile, represented as percent change from baseline NTX versus time. A larger simulation of 1,000 replicates was subsequently conducted with parameter uncertainty as part of a global sensitivity analysis, which has been defined as "a systematic study in which a neighborhood of alternative assumptions is selected and the corresponding interval of inferences is identified" [24]. The global sensitivity analysis utilized the percent change from baseline NTX at 2 weeks post dose as the endpoint of clinical interest. It is important to note that a global sensitivity analysis is simply the result for a time point of interest from the simulation plotted as a function of each fixed effect. The global sensitivity analysis illustrates simulation outcome dependencies on model parameters taken over the uncertainty in all model parameters simultaneously.

A local sensitivity analysis [25] was also conducted for comparison with the global sensitivity analysis. Using a simulation of 1,750 subjects given a SC dose of 3.0 mg/kg, partial derivatives of the model prediction with respect to a given fixed effect parameter were calculated at every time point for every subject. The simulation size was exclusively dictated by memory limitations in the software we used for post-processing of the simulation results. S-Plus 2000 Professional Release 3 (Insightful, Seattle, WA) was used to manipulate and plot all data from analyses and simulations. The partial derivatives of the model prediction with respect to the kth random effect ($\delta F/\delta \eta_k$) were evaluated using the final parameter estimates and simulated data set. To be more specific, these derivatives were accessed using verbatim code after the FSUBS file was analyzed to determine the partial derivative variable names [26]. To calculate

the partial derivatives with respect to the kth parameter ($\delta F/\delta P_k$), the chain rule for partial derivatives was applied. Individual normalized sensitivity indices were then calculated using individual model predictions and their respective parameter values. The normalized sensitivity indices were used to guide the investigation of the global sensitivity analysis.

Results

Pharmacokinetic results

The final PK model consisted of three compartments, with a fourth for first-order absorption of subcutaneously administered Fc-OPG, and both linear and Michaelis–Menten elimination from the central compartment (Fig. 1). This compartmental model structure is described by the following set of differential equations:

$$\begin{aligned}
\frac{dA_1(t)}{dt} &= \frac{Q_2}{V_2}A_2(t) + \frac{Q_3}{V_3}A_3(t) - \left[\frac{Q_2 + Q_3 + CL}{V_C} + \frac{V_{\max}}{K_M V_C + A_1(t)}\right]A_1(t) \\
\frac{dA_2(t)}{dt} &= \frac{Q_2}{V_C}A_1(t) - \frac{Q_2}{V_2}A_2(t) \\
\frac{dA_3(t)}{dt} &= \frac{Q_3}{V_C}A_1(t) - \frac{Q_3}{V_3}A_3(t) \\
\frac{dA_4(t)}{dt} &= -k_a A_4(t)
\end{aligned} \tag{3}$$

where $A_n(t)$ indicates the mass of Fc-OPG in compartment n (1 = serum, 2 = fast equilibrating, 3 = slow equilibrating, 4 = subcutaneous depot), V_C is the central compartment volume of distribution, V_2 and V_3 are the peripheral compartment volumes, Q_p is the intercompartmental clearance between the central compartment and compartment p, CL is the linear clearance from serum, and V_{max} and K_M describe Michaelis–Menten elimination. At t = 0, the initial condition for the mass in each compartment was zero. Subcutaneously injected Fc-OPG was modeled with a first-order absorption rate constant of k_a and a bioavailability of F.

Initial full population model exploration with the comprehensive (IV+SC) data set proved to be an ineffective approach to model selection, as demonstrated in the flow chart of the model building process made available as supplementary material. Estimation runs were characterized by convergence difficulties and unstable or unrealistic fixed effect and random effect parameter estimates. Consequently, it was assumed that the SC data, which demonstrated substantial intersubject variability, did not provide sufficient information for estimation of the structural PK parameters except for the absorption rate constant and bioavailability. The data were therefore separated into two data sets by route of Fc-OPG administration, and the IV data were used in the initial structural model selection process. With superior diagnostic plots and an acceptably lower MOFV at an $\alpha = 0.01$ chi-square distribution level (-463.5 compared to -284.4, 283.8, and 354.3), the three-compartment, parallel elimination model was selected as the structural model of choice. A diagonal OMEGA matrix fitting of

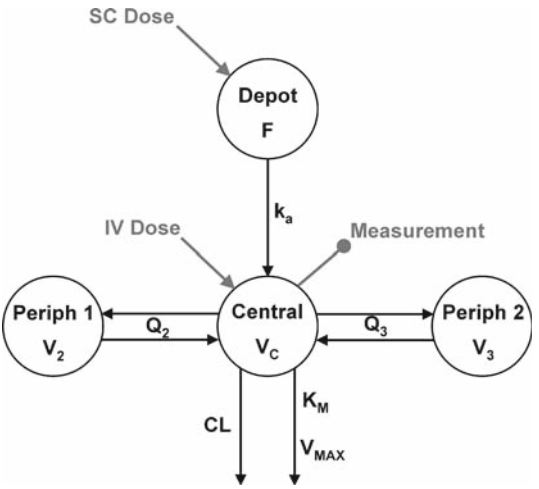

Fig. 1 Final compartmental model for Fc-OPG pharmacokinetics. V_C is the central compartment volume of distribution, V_2 and V_3 are the peripheral compartments' volumes, Q_p is the intercompartmental clearance between the central compartment and compartment p, CL is the linear clearance from serum, and V_{max} and K_M describe Michaelis–Menten elimination. Subcutaneously injected compound had a first-order absorption rate of k_a and a bioavailability of F. See text for more details

this model with random effects on all parameters (eight nonzero OMEGA elements), however, resulted in a failure to obtain the asymptotic covariance matrix of the estimates, and further investigation into the OMEGA matrix structure was therefore conducted. As a strategy for building a parsimonious OMEGA matrix structure, we followed a stepwise approach to selecting the final set of intersubject error terms.

In conclusion, only five of the eight IV model parameters retained intersubject variance terms. Specifically, random effects were applied to the three volume terms (V_C, V_1, V_2), one inter-compartmental clearance (Q_2), and the central compartment clearance (CL). All other fixed effects (Q_3, K_M, and V_{MAX}) were estimated without intersubject variability, and thus, were held constant for the population. This model, with five independent random effects, demonstrated improved goodness of fit when compared to models with less OMEGA elements, while all models with more random effect terms did not meet the applied selection criteria. Also, a covariance matrix of parameter estimates became unavailable for all models after more than five terms were added to the OMEGA matrix. Therefore, five intersubject variance terms were retained and estimated. The model goodness-of-fit diagnostic plots for the final IV PK data are shown in Fig. 2.

With all random and fixed effects parameters fixed to their final estimated values, based on IV data analysis (see Table 1), two additional fixed effect parameters (F and k_a) and three additional random effect parameters (ω^2_F, ω^2_{ka}, ω^2_{F-ka}) were fit to the SC data using a first-order absorption compartment. SC proportional residual error variance was estimated separately from the IV residual error variance. These parameter estimates are included in Table 1, along with their estimated standard errors. Diagnostic plots and population model fitting are shown in Fig. 3.

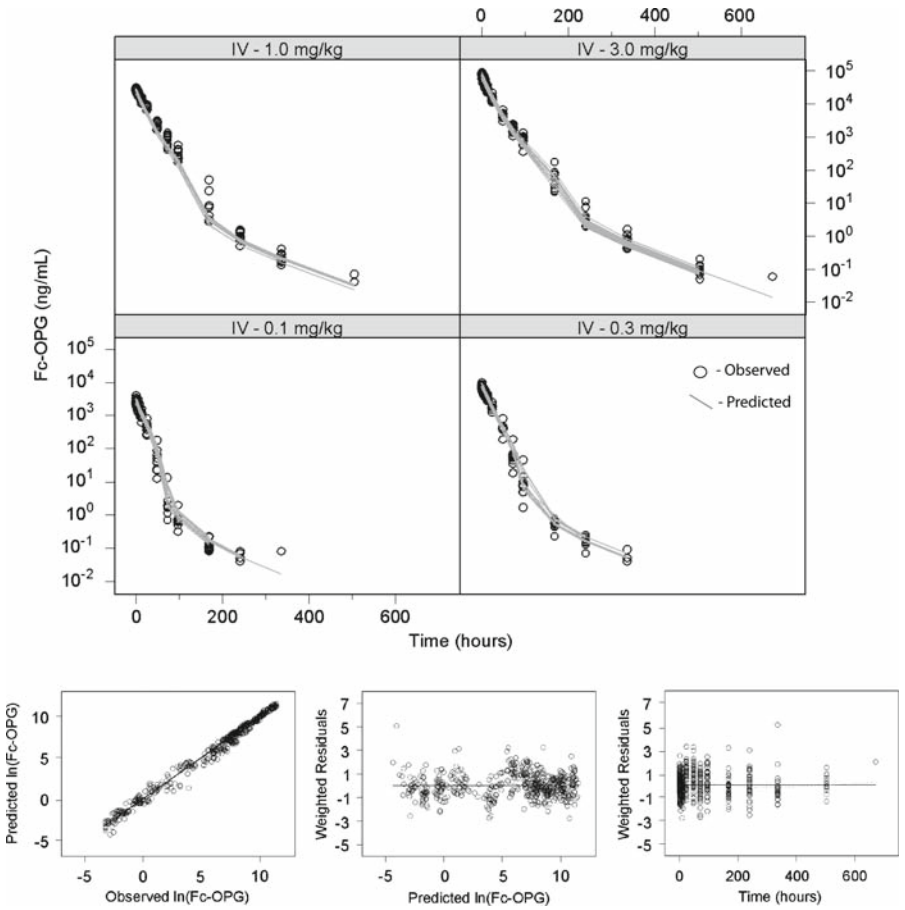

Fig. 2 PK model diagnostic plots for IV administered compound. Predicted and observed concentrations have been log-transformed for analysis. The four-panel plot shows typical population model predicted Fc-OPG serum concentration (PRED) and observed Fc-OPG serum concentration (DV) on a log scale versus elapsed time after injection (TIME) (by cohort) on a log scale. The three diagnostic plots are (from left to right): PRED versus DV; weighted residuals of model prediction (WRES) versus PRED; WRES versus TIME. For all plots except PRED and DV versus TIME, the solid line represents a perfect model fit, and the dotted line is the Loess fit of the plot data points. For the PRED and DV versus TIME graph, the continuous line is the typical population model predicted fit to the IV data points

Pharmacodynamic results

The PD model structure is described by the following indirect response equation:

$$\frac{dNTX(t)}{dt} = k_{syn}\left(1 - \frac{I_{MAX}C_{OPG}(t)}{IC_{50} + C_{OPG}(t)}\right) - k_{\text{deg}}NTX(t) \tag{4}$$

where k_{syn}, k_{deg}, and IC_{50} are the PD model parameters, $C_{OPG}(t)$ is the PK model-predicted Fc-OPG serum concentration (ng/ml), and NTX(t) is the predicted value of

Table 1 Final population PK model parameters (fixed and random effects), including % relative standard error

Model Parameter (units)	Definition	Estimated value	% Relative standard error
K_M (ng/ml)	Michaelis–Menten constant of nonlinear clearance	6.74	11
V_{MAX} (ng/h)	Maximum velocity of nonlinear clearance	13,300	13
V_C (ml)	Central compartment volume of distribution	2,800	2
V_2 (ml)	Peripheral compartment 2 volume of distribution	443	16
V_3 (ml)	Peripheral compartment 3 volume of distribution	269	14
CL (ml/h)	Linear clearance	168	3
Q_2 (ml/h)	Intercompartmental clearance between central and peripheral compartment 2	15.5	16
Q_3 (ml/h)	Intercompartmental clearance between central and peripheral compartment 2	3.02	13
F (unitless)	Bioavailability fraction	0.0719	9
k_a (h^{-1})	Absorption rate constant	0.0131	4
ω^2_{VC}	Intersubject variance of central V_c	0.0102	39
ω^2_{V2}	Intersubject variance of V_2	0.0144	52
ω^2_{V3}	Intersubject variance of V_3	0.0333	124
ω^2_{CL}	Intersubject variance of CL	0.0391	20
ω^2_{Q2}	Intersubject variance of Q_2	0.0379	71
ω^2_{F}	Intersubject variance of F	0.263	20
ω^2_{ka}	Intersubject variance of k_a	0.0457	31
cov_{F-ka}	Covariance of F and k_a		48
σ^2_{IV}	Residual error variance following IV administration of Fc-OPG	0.0193	13
σ^2_{SC}	Residual error variance following SC administration of Fc-OPG	0.733	11

urinary NTX. The initial condition for NTX was defined as the ratio of k_{syn} to k_{deg} with the individual predose values fitted. The three fixed effects parameter estimates and corresponding inter-individual variance estimates are listed in Table 2, which also includes estimates of the covariance between k_{syn} and k_{deg} and proportional and additive residual error variances. Diagnostic plots for the population prediction for this model are shown in Fig. 4, with the individual model predictions overlaid on the raw data. The plot of observed versus population predicted values show a fixed ceiling and appear to show a poor fit. However, this ceiling is due to the population estimate of baseline urinary NTX, which is highly variable (as seen in the plot of individual model predictions in Fig. 4). Figure 5 shows the population model prediction fit to the raw data,

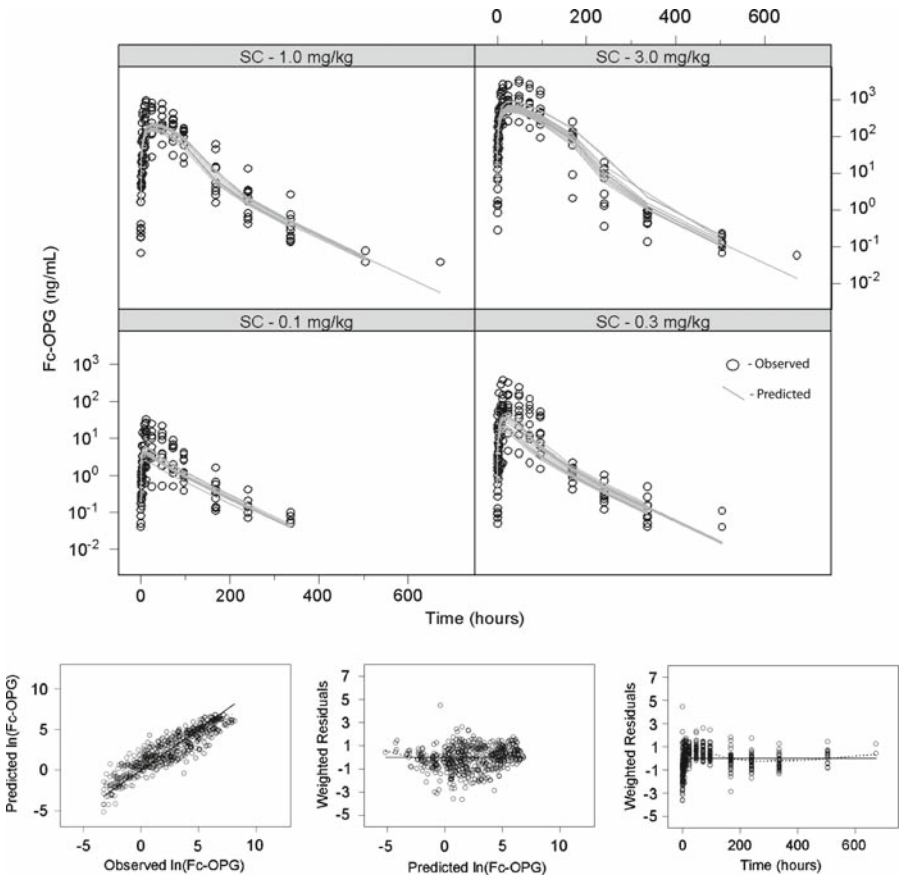

Fig. 3 PK model diagnostic plots for SC administered compound. Predicted and observed concentrations have been log-transformed for analysis. The four-panel plot shows typical population model predicted Fc-OPG serum concentration (PRED) and observed Fc-OPG serum concentration (DV) on a log scale versus elapsed time after injection (TIME) (by cohort). The other three diagnostic plots are (from left to right): PRED versus DV; weighted residuals of model prediction (WRES) versus PRED; WRES versus TIME. For all plots except PRED and DV versus TIME, the solid line represents a perfect model fit, and the dotted line is the Loess fit of the plot data points. For the PRED and DV versus TIME graph, the continuous line is the typical population model predicted fit to the SC data points

and does not capture the spread in NTX baseline. It is also important to note that we assumed that I_{MAX} was 100% in this equation to minimize the number of estimated parameters. An expanded model where I_{MAX} was an estimated parameter caused rounding errors and did not drastically change the values of the other PD parameters (I_{MAX} was estimated as ~ 0.89). The noticeable underestimation of low urinary NTX values (Fig. 4) may be attributed to a high I_{MAX}; however, due to model instability when fitting this parameter, we chose to fix it at maximum inhibition. Another explanation as to why the lower NTX values seem to be underestimated may be due to a possible covariate effect that was either unavailable from the study or was not included.

Table 2 Final population PD model parameters (fixed and random effects), including % relative standard error

Model Parameter (units)	Definition	Estimated value	% Relative standard error
k_{syn} ([nM BCE/mM creatinine]/h)	Biomarker synthesis rate	0.864	8
k_{deg} (h^{-1})	Biomarker elimination rate constant	0.0204	6
IC_{50} (ng/ml)	Half-maximal inhibitory concentration	5.38	21
ω^2_{ksyn}	Intersubject variance of k_{syn}	0.281	28
ω^2_{kdeg}	Intersubject variance of k_{deg}	0.0325	88
$Cov_{ksyn-kdeg}$	Covariance of k_{syn} and k_{deg}	0.0867	59
ω^2_{IC50}	Intersubject variance of IC_{50}	1.18	43
σ^2_{prop}	Proportional residual error variance of biomarker	0.0407	13
σ^2_{add}	Additive residual error variance of biomarker	20.7	19

Posterior predictive check

Figure 6 shows the observed population median and simulated distribution of population medians for the natural logarithm of Fc-OPG serum concentrations, NTX, and the percent change from baseline NTX at 2 weeks after dosing by cohort. In each plot, the distribution of the simulated population median adequately captures the observed population median for the PK and PD models. A single exception is the percent change from baseline NTX in cohort 8, where the highest IV dose was administered, in which the simulated distribution does not accurately reflect the actual median of the normalized data. This result may be due to the small sample population per cohort (n = 10 subjects/cohort), and may be further explained by considering the additional error involved in calculating a derived normalized metric such as percent suppression. As error is present on both post-dose and baseline NTX values, when the ratio is taken, the errors are amplified. In addition, there seems to be a trend towards model overprediction with increasing dose. Yet, it is also apparent that the results of the posterior predictive check for the measured dependent variables Fc-OPG and NTX are acceptable. These results support further use of the model and the estimated parameters in predictive simulations of these and other dosing schemes in larger populations.

Predictive simulations and sensitivity analyses

Figure 7 summarizes the simulated distribution of NTX percent change from baseline over time for a population of 200 subjects reflecting a SC dosing scheme at 3.0 mg/kg. Only 200 replicate simulations were performed to obtain this plot, due to computer memory limitations. The population median percent NTX suppression for all 200 simulations had a 95% uncertainty interval of [−34%, −60%] at 2 weeks. The median

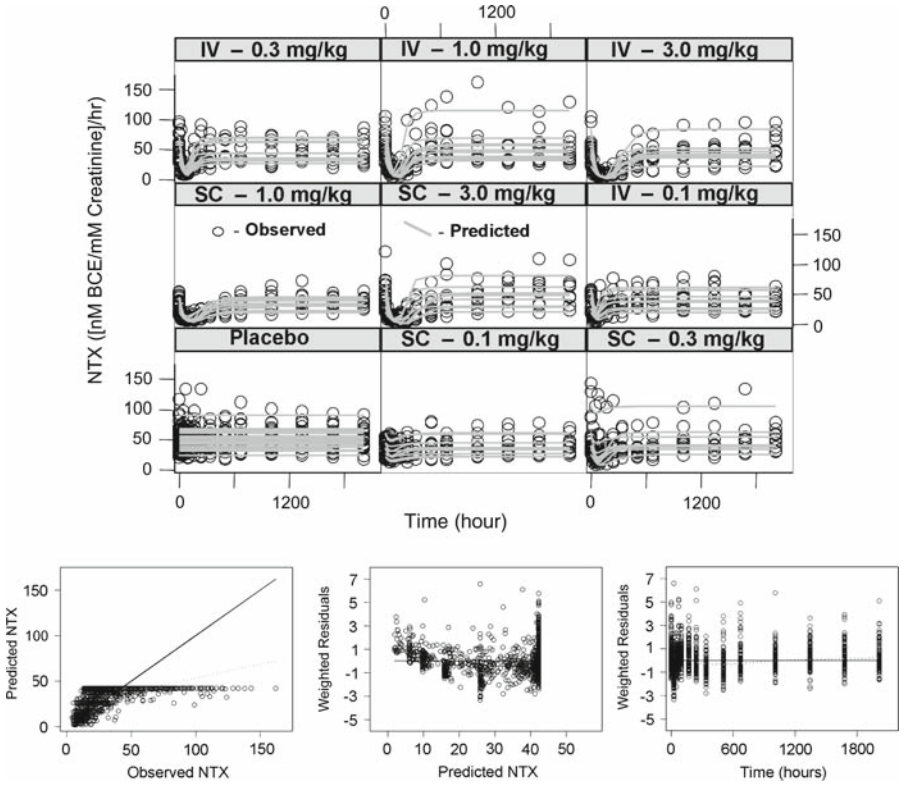

Fig. 4 PD model diagnostic plots. The nine-panel plot shows individual model predicted (IPRED, instead of typical population model predicted concentrations, PRED, as in Figs. 3 and 4) and observed urinary NTX values (DV) versus elapsed time after injection (TIME) (by cohort; note that we added an additional plot which shows all the placebo subjects). The other three diagnostic plots are (from left to right): PRED versus DV; weighted residuals of model prediction (WRES) versus PRED; WRES versus TIME. For all plots except IPRED and DV versus TIME, the solid line represents a perfect model fit, and the dotted line is the Loess fit of the plot data points. For the PRED and DV versus TIME graph, the continuous line is the typical population model predicted fit to the IV data points

prediction interval for percent suppression at 2 weeks among all trials was [8.5%, −93.7%]. This large variance, however, is not just due to uncertainty in the simulation outcome, but reflects the observed large intersubject variability clearly seen in the raw SC data (Figs. 3 and 4 [SC panels]).

To evaluate the global sensitivity of the prediction provided by the PK–PD model to assumptions about parameter estimates, 1,000 simulations of the same trial (3.0 mg/kg, 200 subjects) were performed, including uncertainty in all parameter estimates. For each trial, the simulated outcome (2-week NTX percent suppression) was plotted as a function of the corresponding simulated population parameter for that trial. Parameters that have, on average, more influence on the outcome will exhibit a stronger relationship between the outcome and parameter values. In this context, sensitivity to parameter uncertainty can be viewed as a positive or negative trend between the 2-week NTX percent suppression versus the typical population parameter value across

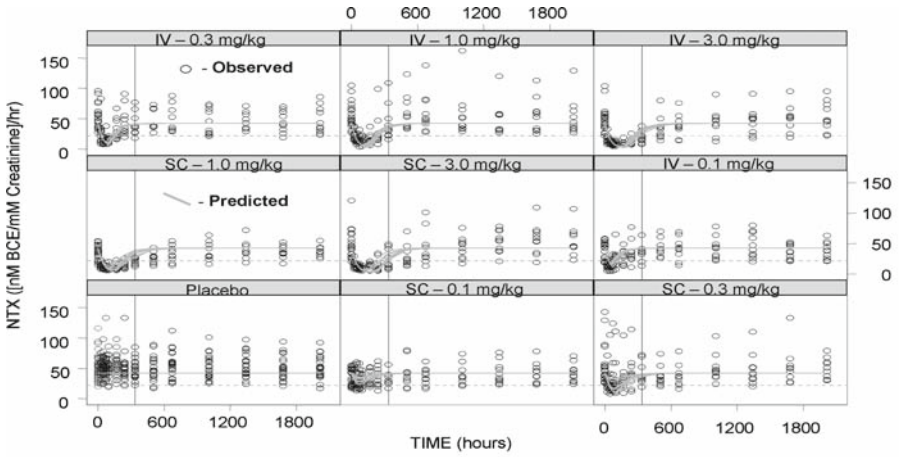

Fig. 5 Typical population model predicted (PRED) versus observed NTX values (DV) split by cohort, with an additional plot (bottom left) showing all cohorts placebo subjects. To design our simulations, we looked at doses that achieved average 50% suppression from baseline NTX at 2 weeks. This occurrence is represented by the intersection of the 2 week time point (marked by the solid vertical line in all plots) and the average 50% suppression from baseline NTX (dotted horizontal line). Based on this reasoning, dosing in Cohort 4 was chosen for our simulations

all 1,000 trial replicates. Figure 8 uses a Loess smoothing curve and 95% confidence interval to display the global sensitivity of the 2-week PD endpoint to various fixed effect parameters (S-Plus "locfit" library). Of the 13 fixed effect parameters, only 5 noticeably impacted the simulation outcome (IC_{50}, F, V_{MAX}, k_a, and K_M). Despite a few strong sensitivities to parameter estimates, the overall simulation outcome uncertainty is fairly low, as indicated in Fig. 7. A local sensitivity analysis was also performed on both the PK and PD models. As opposed to global sensitivity, local sensitivities display the sensitivity of the computed model output over time to small changes in one parameter value at a time. Selected results are displayed in Fig. 9. Only local sensitivity plots for the PD model outcome are included for comparison to the global sensitivity plots. Further, we display only those parameters that showed elevated local sensitivities in one or more regions of the plot. Again, the normalized sensitivity indices are used to direct the global sensitivity analysis.

Discussion

This report describes the PK and PD analysis of IV and SC data of the RANKL inhibitor, Fc-OPG, from a study performed in healthy postmenopausal women. It further describes the subsequent evaluation of the resulting PK and PD models using a posterior predictive check, and suggests how such models can be used to conduct simulations of clinical trials. The uncertainty in the clinical trial simulations and sensitivity of the simulation results to parameter assumptions were also evaluated. Although the derived PK–PD model was specific to Fc-OPG, the model development, evaluation, and

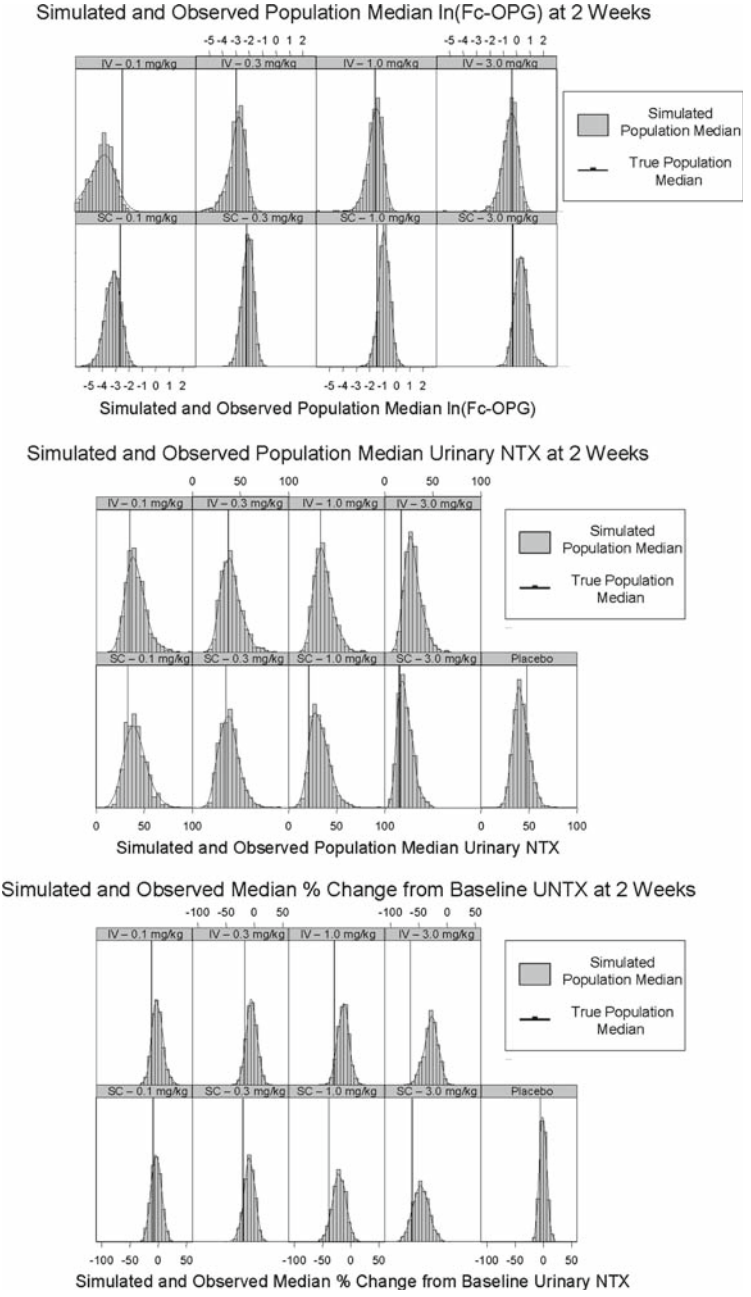

Fig. 6 Posterior predictive check plots. From top to bottom: Fc-OPG log-transformed concentration (eight cohorts); NTX values (eight cohorts with placebo); percent change from baseline NTX (eight cohorts with placebo). The plots show the distribution of simulated population median values (histogram; 1,000 populations) and actual population median from the available data (vertical line) at 2 weeks post drug administration

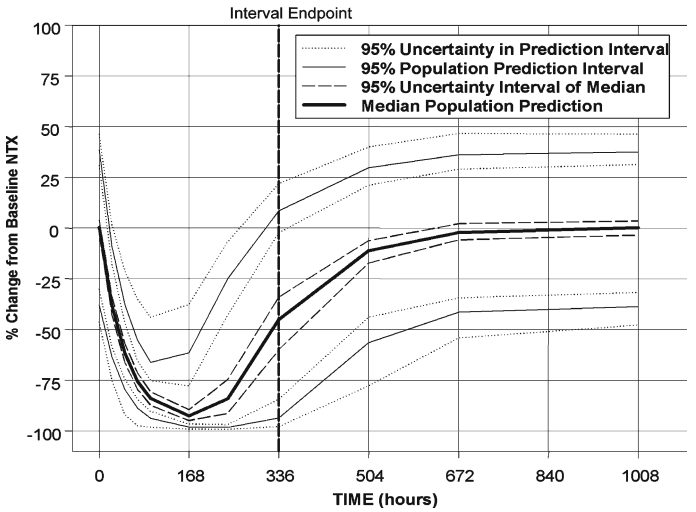

Fig. 7 Simulation of 200 replicate trials, each with 200 subjects, based on a single SC dose of 3 mg/kg, reflecting cohort 4 dosing in the original data set (body mass was assumed to be 70 kg for all subjects). The thick solid line represents the median value of all median NTX percent changes from baseline (across the 200 simulated trials; one median value is obtained from each simulated trial). The dashed lines delimit the 95% uncertainty interval for the population median value. The thin solid lines show the median values of all 95% population variability prediction intervals (across the 200 simulated trials). The dotted lines show the 95% uncertainty interval in the population 95% prediction intervals. The vertical dashed line intersects the computed profiles at 2 weeks after drug administration, and it helps to gauge visually how effective a biweekly dosing regimen might be. See text for further details

simulation processes described here could easily be generalized to other complex PK–PD systems.

The PK and PD parameters obtained by the model fitting (described in Tables 1 and 2) were within a reasonable physiological range. Furthermore, a posterior predictive check of selected model predictions (Fc-OPG, NTX, and % suppression NTX) showed accurate model descriptions of these endpoints in postmenopausal women. In fact, the posterior predictive check showed a range of simulated median outcomes that contained the actual data median with high probability in all but a single case. These results indicate that this PK–PD model may be an effective tool for simulating an Fc-OPG clinical trial or for exploring the drug's effects under various dosing scenarios.

Focusing on cohort 4 (3.0 mg/kg, SC) as a possible clinically effective dosing regimen, the expected percent suppression of NTX over time for a trial of 200 subjects was simulated using estimated model parameters. The simulation results were encouraging, as the overall uncertainty of the median outcome was fairly small. The parameters most influential to the simulation outcome were detected in the global sensitivity analysis. Specifically, the global sensitivity analysis revealed noticeable relationships between percent suppression and typical population parameters for IC_{50}, F, V_{MAX}, k_a, and K_M. Given these strong dependencies, it may be important to quantify these parameters as accurately as possible by gathering additional information to limit uncertainty in

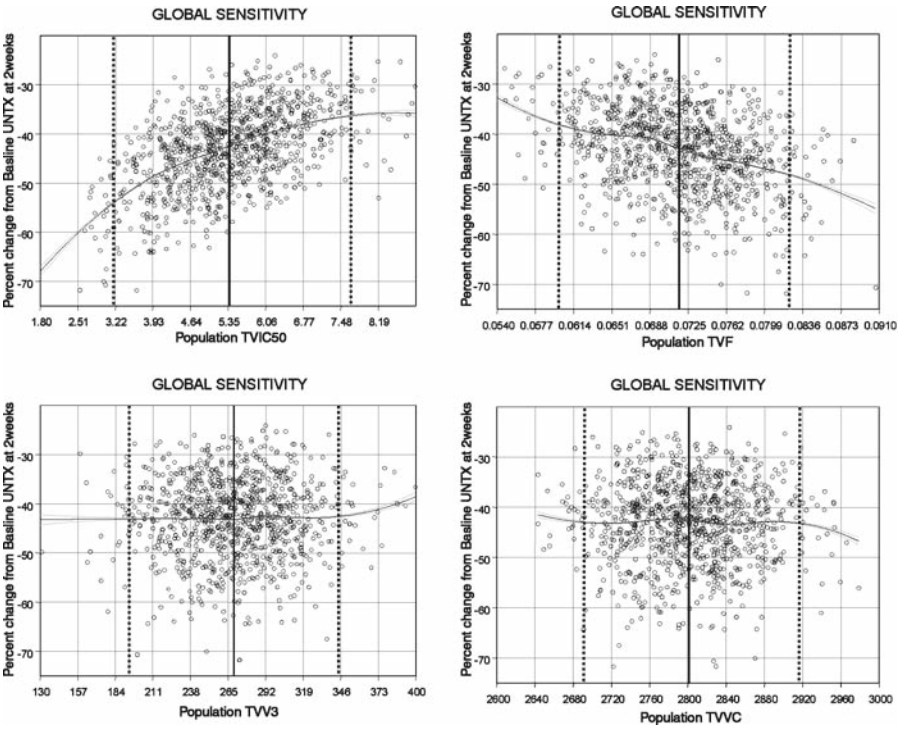

Fig. 8 Global sensitivity analysis results. Clockwise from top left, global sensitivity plots for IC_{50}, F, V_C and V_3 are shown. The simulation outcome is highly sensitive to uncertainty in the model parameters IC_{50} and F, for example, while sensitivity to uncertainty in V_C and V_3 is negligible. All plots show NTX percent change from baseline versus the typical value of the population parameter (TV*par* in the plots). The open circles show a scatter plot of the simulated predictions together with a Loess-fit curve and its 95% confidence interval (solid lines). The vertical thick line is the final typical value estimate from the original PK or PD model and the vertical red lines represent the 95% uncertainty interval for that parameter estimate (from the NONMEM asymptotic covariance matrix). The steeper the slope of the Loess-fit curve, the more sensitive the simulated outcome is to that particular parameter estimate. These plots were obtained for all 13 fixed effect parameters, and only 5 displayed noticeable sensitivity (IC_{50}, F, V_{MAX}, ka, and K_M)

overall predictions. It should also be noted, however, that the less influential parameters (from global sensitivity analysis) may not need to be estimated with strict certainty, as their values have little impact on the overall simulated clinical outcome. Thus, the sensitivity analysis indicates where to concentrate resources for future studies, if necessary.

The results of the 200-subject, 3.0-mg/kg, SC simulations showed a low overall uncertainty in population median percent suppression after 2 weeks, with a 95% uncertainty interval of $[-34\%, -60\%]$. If the influential parameters could be estimated with increased precision the uncertainty interval would correspondingly decrease. Nonetheless, at the current level of uncertainty in the outcome prediction, decisions about the utility of this dosing regimen could be made with a sufficient degree of confidence. Thus, considering that Fc-OPG produced rapid NTX suppression that was similar to or greater than the median for the bisphosphonate residronate, and NTX suppression

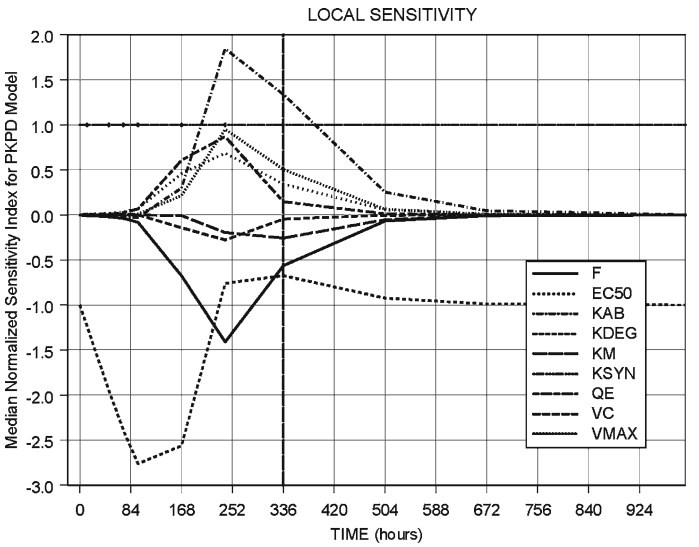

Fig. 9 Local sensitivity analysis. The continuous lines show the value of the median (across one population of 1,750 subjects) normalized sensitivity index for the PD outcome over time for various PK and PD parameters. A value of 1.0 on the ordinate corresponds to 100% normalized sensitivity. The vertical dashed line pinpoints the time (2 weeks after administration) at which the global sensitivity analysis was performed. In contrast to the global sensitivity analysis, this plot shows sensitivity of model predicted NTX values to PK–PD parameters, while the global analysis uses percent change in NTX from baseline as the simulated outcome

is reported in the literature to correlate with increases in bone mineral density and decreases in risk of vertebral fractures, it appears that this dose and regimen would be desirable to carry forward to subsequent clinical trials [27]. The 2-week clinical outcome chosen here, however, is somewhat arbitrary, although supported by the literature on osteoporosis treatments, and a global sensitivity analysis at a different time may have different parameter sensitivities. This can be observed in the local sensitivity analysis (Fig. 9). Although the normalized sensitivity indices do not take uncertainty in parameter estimation into account, they show how the population model mean prediction depends on single fixed effect parameter estimates over time. Thus, the local sensitivity analysis may be used as a prediction of simulation outcome sensitivity for other timepoints.

We believe that the model development and evaluation exercise performed here is important for many reasons. It should not be overlooked that model development began by pooling all subjects' data to determine an initial structural model. The naïve pool approach can dramatically reduce the time it takes to select the basic model (differential equation) structure and should provide accurate parameter estimates when the study design is characterized by balanced sampling across individuals. Moving on to population analysis, the selection of between-individual variance terms included in the model was developed in a fashion similar to approaches commonly used for covariate model building. The model development process was also aided by a piecewise model-building approach which separated IV and SC data, to avoid the poor estimates we observed

when fitting the model to all the available data together. The resulting population PK–PD model was then evaluated using a posterior predictive check. Using the standard errors predicted by NONMEM's $COVARIANCE step, the simulation included uncertainty in the population parameter estimates (implemented as inter-trial variability). The evaluation performed here allows one to quickly ascertain relevant conclusions about the range of possible outcomes by taking advantage of all available information and by acknowledging the current level of knowledge about the system. The global sensitivity analysis then exposes those parameters whose uncertainty may greatly influence the predicted clinical outcome. This information then can be used to explore the current understanding and assumptions regarding the dose and regimen selection.

In conclusion, consistent with modeling work reported to date in the field of osteoporosis with other antiresorptive treatments, the development of informative PK–PD models may improve the confidence in selected regimens and doses and reduce the number of uninformative or failed trials. Dose and regimen selection is critical especially in this therapeutic area, which requires at least 3-year trials with thousands of patients to obtain a statistically significant signal in a fracture outcome. Lastly, the approach taken here is easily generalizable and can be applied to a wide variety of compounds without compromising its value.

Acknowledgements This work was funded by Amgen, Inc., and partially supported by NIH grant P41 EB-001975.

References

1. Akesson K (2003) New approaches to pharmacological treatment of osteoporosis. Bull World Health Organ 81:657–664
2. Ettinger MP (2003) Aging bone and osteoporosis: strategies for preventing fractures in the elderly. Arch Intern Med 163:2237–2246. doi:10.1001/archinte.163.18.2237
3. Sitruk-Ware R (2003) Alternatives for optimal hormone replacement therapy. Climacteric 6(Suppl 2):11–16
4. Draper MW (2003) The role of selective estrogen receptor modulators (SERMs) in postmenopausal health. Ann N Y Acad Sci 997:373–377. doi:10.1196/annals.1290.040
5. Rubin MR, Bilezikian JP (2003) The anabolic effects of parathyroid hormone therapy. Clin Geriatr Med 19:415–432. doi:10.1016/S0749-0690(02)00074-5
6. Boyle WJ, Simonet WS, Lacey DL (2003) Osteoclast differentiation and activation. Nature 423:337–342. doi:10.1038/nature01658
7. Hofbauer LC, Kuhne CA, Viereck V (2004) The OPG/RANKL/RANK system in metabolic bone diseases. J Musculoskelet Neuronal Interact 4:268–275
8. Bekker PJ, Holloway D, Nakanishi A, Arrighi M, Leese PT, Dunstan CR (2001) The effect of a single dose of osteoprotegerin in postmenopausal women. J Bone Miner Res 16:348–360. doi:10.1359/jbmr.2001.16.2.348
9. Colburn WA (2003) Biomarkers in drug discovery and development: from target identification through drug marketing. J Clin Pharmacol 43:329–341. doi:10.1177/0091270003252480
10. Gobburu JV, Sekar VJ (2002) Application of modeling and simulation to integrate clinical pharmacology knowledge across a new drug application. Int J Clin Pharmacol Ther 40:281–288
11. Meibohm B, Derendorf H (2002) Pharmacokinetic/pharmacodynamic studies in drug product development. J Pharm Sci 91:18–31. doi:10.1002/jps.1167
12. Holford NH, Kimko HC, Monteleone JP, Peck CC (2000) Simulation of clinical trials. Annu Rev Pharmacol Toxicol 40:209–234. doi:10.1146/annurev.pharmtox.40.1.209

13. Blesch KS, Gieschke R, Tsukamoto Y, Reigner BG, Burger HU, Steimer JL (2003) Clinical pharmacokinetic/pharmacodynamic and physiologically based pharmacokinetic modeling in new drug development: the capecitabine experience. Invest New Drugs 21:195–223. doi:10.1023/A:1023525513696
14. Gomeni R, Dangeli C, Bye A (2002) In silico prediction of optimal in vivo delivery properties using convolution-based model and clinical trial simulation. Pharm Res 19:99–103. doi:10.1023/A:1013667718695
15. Nestorov I, Graham G, Duffull S, Aarons L, Fuseau E, Coates P (2001) Modeling and stimulation for clinical trial design involving a categorical response: a phase II case study with naratriptan. Pharm Res 18:1210–1219. doi:10.1023/A:1010943430471
16. Research, USDoHaH, Administration, FaD, (CDER), CfDEaR & (CBER), CfBEaR guidance for industry population pharmacokinetics (1999)
17. Pillai G, Gieschke R, Goggin T, Jacqmin P, Schimmer RC, Steimer JL (2004) A semimechanistic and mechanistic population PK–PD model for biomarker response to ibandronate, a new bisphosphonate for the treatment of osteoporosis. Br J Clin Pharmacol 58:618–631. doi:10.1111/j.1365-2125.2004.02224.x
18. Cremers S, Sparidans R, den HJ, Hamdy N, Vermeij P, Papapoulos S (2002) A pharmacokinetic and pharmacodynamic model for intravenous bisphosphonate (pamidronate) in osteoporosis. Eur J Clin Pharmacol 57:883–890. doi:10.1007/s00228-001-0411-8
19. Beal SL, Sheiner LB (1992) NONMEM User Guide. In: NONMEM Project Group. University of California San Francisco, San Francisco
20. Steimer JL, Mallet A, Golmard JL, Boisvieux JF (1984) Alternative approaches to estimation of population pharmacokinetic parameters: comparison with the nonlinear mixed-effect model. Drug Metab Rev 15:265–292. doi:10.3109/03602538409015066
21. Carroll RJ, Ruppert D (1988) Transformation and weighting in regression. CRC Press
22. Jonsson EN, Karlsson MO (1999) Xpose–an S-PLUS based population pharmacokinetic/pharmacodynamic model building aid for NONMEM. Comput Methods Programs Biomed 58:51–64. doi:10.1016/S0169-2607(98)00067-4
23. Yano Y, Beal SL, Sheiner LB (2001) Evaluating pharmacokinetic/pharmacodynamic models using the posterior predictive check. J Pharmacokinet Pharmacodyn 28:171–192. doi:10.1023/A:1011555016423
24. Leamer EE (1990) Sensitivity analysis would help. In: Granger CWJ (ed) Modelling Economic Series. Clarendon Press, Oxford
25. Nestorov IA (1999) Sensitivity analysis of pharmacokinetic and pharmacodynamic systems: I. A structural approach to sensitivity analysis of physiologically based pharmacokinetic models. J Pharmacokinet Biopharm 27:577–596. doi:10.1023/A:1020926525495
26. Piotrovskij V, Van Peer A (1997) A model with separate hepato-portal compartment ("first-pass" model): fitting to plasma concentration-time profiles in humans. Pharm Res 14:230–237. doi:10.1023/A:1012065130597
27. Eastell R, Barton I, Hannon RA, Chines A, Garnero P, Delmas PD (2003) Relationship of early changes in bone resorption to the reduction in fracture risk with risedronate. J Bone Miner Res 18:1051–1056. doi:10.1359/jbmr.2003.18.6.1051